Fiber bundles with integrated bandpass and notch filters for in-vivo Raman spectroscopy

John Barton, Gary Carver, Sheetal Chanda, Sarah Locknar, Manish Gupta

Proc. SPIE 11233, Optical Fibers and Sensors for Medical Diagnostics and Treatment Applications XX, 112330S (20 Feb 2020);

https://doi.org/10.1117/12.2546207

Fiber bundles with integrated bandpass and notch filters for in-vivo Raman spectroscopy

John Barton, Gary Carver*, Sheetal Chanda, Sarah Locknar
Omega Optical Inc.
Brattleboro, VT 05301

Manish Gupta
Nikira Labs Inc.
Mountain View, CA 94043

ABSTRACT

Raman spectroscopy is used in many areas including pharmaceuticals, geology, chemical engineering, semiconductors, and the life sciences. More recently, Raman fiber sensors have been developed for minimally invasive applications in clinical histopathology. This paper describes the modeling, fabrication, and testing of filters directly deposited onto the excitation and collection fiber tips of a Raman probe. The narrow spectral width of laser rejection filters on the collection fibers should allow for the detection of low wavenumber Raman scattering within the "fingerprint" region. Deep blocking of the laser radiation is enabled by coating both ends of the collection fibers.

Keywords: Optical filters, Raman spectroscopy, Coated fiber tips, Clinical histopathology

1. INTRODUCTION

Raman spectroscopy has found use in many disciplines from pharmaceutical analysis to geology to powder testing and life science. More recently, Raman fiber sensors have been developed for minimally invasive applications in clinical histopathology. It is a valuable technique because it has the resolution to definitively identify the chemical composition of a sample surface in a non-destructive manner. One barrier to widespread use in biomedical applications is the lack of a compact fiber-based probe. Development of such a device would enable the technique to be applied through a biopsy needle, an endoscope or arthroscope for surgical monitoring or optical biopsy. Currently available probes are generally of the type illustrated in Figure 1a, which consists of a fiber delivery system with a small package containing free-space optics including focusing optics and several small filters. This basic design has also been integrated into a barrel package down to ½" diameter. A more versatile design would combine excitation and emission into a straight-path configuration integrated directly into a fiber bundle with a diameter of 1 mm (Figure 1b).

In Raman Spectroscopy, a laser beam is pointed at the material of interest and a portion of the light interacts with the sample to cause a wavelength shift corresponding to vibrational modes in the material. The pattern of shifting wavelengths and intensities are unique to each compound. For biological applications, there are 3 main regions of interest in the Raman spectrum. The 2800-3400 cm^{-1} region is rich in C-H stretch bands (primarily lipids), the 1600-1800 cm^{-1} region is rich in C=O and C=C stretch bands (amino acids). The third "fingerprint region" ranges from 500-1500 cm^{-1} and includes a number of combination bands including bends, wags, rocks, and other vibrational modes. The peaks in the fingerprint

* gcarver@omegafilters.com; phone 1 802 251-7346; www.omegafilters.com

region tend to be small, but are instrumental in positively identifying a material. The number of Raman-shifted photons is about 1,000,000x smaller than those reflecting directly off of the sample without shifting (elastically scattered). As a result, to visualize the Raman signal, the elastic laser wavelength needs to be attenuated with an optical density of 6 at a minimum. Further, the Raman-shift can be to higher (Stokes) or lower (anti-Stokes) wavelengths relative to the elastically-scattered laser wavelength. The Stokes signal tends to be stronger, but it can be contaminated by fluorescence emission which causes an underlying broad background signal, especially when UV and visible wavelength lasers are used. A notch filter can be used to detect both Stokes and anti-Stokes signals simultaneously. Detection of both Stokes and anti-Stokes signals have been implemented in specialized experiments (Kauffmann, et al. 2019). When using fiber bundles for delivery of the laser light, Raman signals from the glass used in the fiber makes its way to the sample, broadening the effective laser wavelength. In fact, fiber-based Raman amplifiers are common in telecom - scattering laser light over 40 THz to about 1334 cm^{-1} (Singh, et al. 2007). A narrow-band laser-cleanup filter is therefore required to remove laser sidebands and the fiber Raman signal. This band-pass must be applied to the distal end of the probe (nearest the sample). These bandpass and notch filters are depicted in figure 1B.

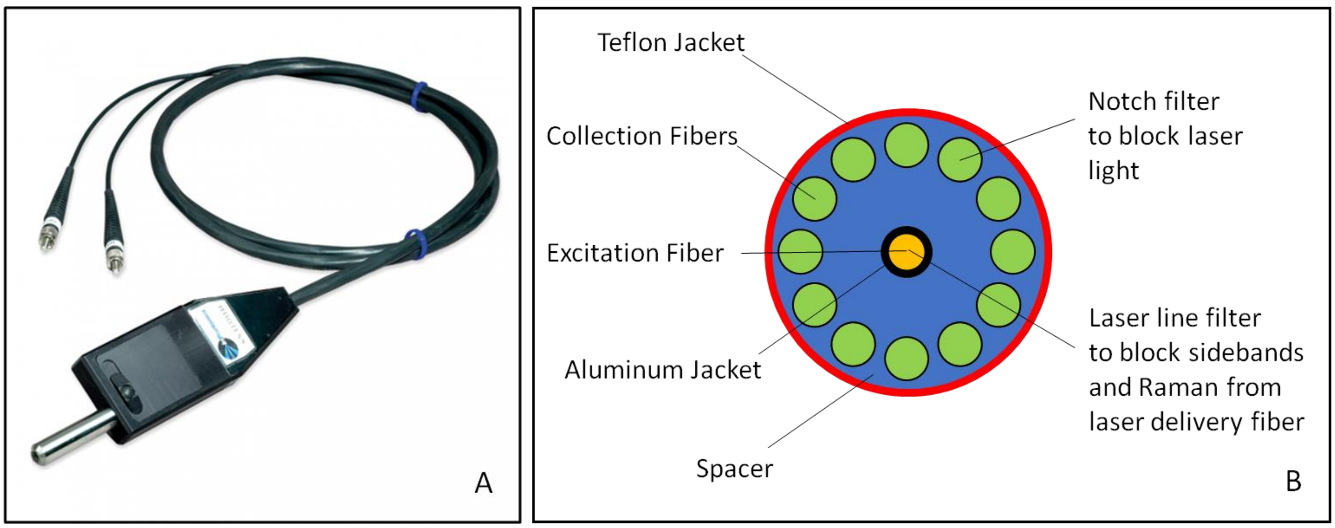

Figure 1A. A commercially available Raman probe consists of a laser delivery fiber and Raman detection fiber with free-space filters in a small package. **B.** The distal end of a fiberoptic bundle that incorporates filtering onto the face of the fiber bundle being developed by Omega Optical and Nikira Labs. The middle fiber delivers laser light while the annular fibers collect Raman signal. Different thin-film filters are applied to each.

The work presented here is early in our process of creating this fiber bundle. We have successfully applied narrow band-pass and notch filters to individual fibers and are working towards an integrated bundle. This paper describes the modeling, fabrication, and testing of filters that can be directly deposited onto the excitation and collection fiber tips of a Raman probe. We will discuss angle-dependent design issues resulting from using the large multi-mode core fibers required for efficient signal collection.

2. OPTICAL DESIGNS

The spectral width of filters on the excitation and collection fibers should allow for the detection of low wavenumber scatter. For strong signal-to-noise, the collection fibers in a Raman probe must have large multimode cores. This leads to a numerical aperture of about 0.22, which means that light encounters the coated fiber tip at angles of incidence (AOI) from zero to about 12 degrees. The designs shown in figures 2 and 3 were computed using standard thin film modeling software. Models are shown for the bandpass and notch in each figure, wherein figure 2 is for deposition in an electron-beam (e-beam) evaporation system and figure 3 is for deposition in a magnetron sputtering system. Due to delamination issues, our e-beam depositions are limited to a total physical thickness of about 7 microns. The bandpass in figure 2 is composed of two Fabry-Perot cavities including 13 layers of ZnS and YF totaling a physical thickness of 4 microns. The notch in figure 2 is composed of 66 layers of ZnS and ZnSe totaling a physical thickness of 5.5 microns. Our sputtering process allows for thicker depositions with robust adherence. The bandpass in figure 3 is composed of four Fabry-Perot cavities (plus four more shallow cavities for blocking) including 72 layers of Nb_2O_5 and SiO_2 totaling a physical thickness of 9 microns. The notch in figure 3 is composed of 170 layers of Nb_2O_5 and SiO_2 totaling a physical thickness of 16 microns. The figures show models for an AOI of zero degrees, while the fiber NA distributes power from zero to 12 degrees. The curves will shift about 4 nm to the blue at 12 degrees. Data described in section 4 indicates that the integrated AOI effect on bandshape is closer to zero than the 12 degrees. Curves in each figure are included for doubling the notch OD to provide deep blocking by coating both ends of the collection fibers.

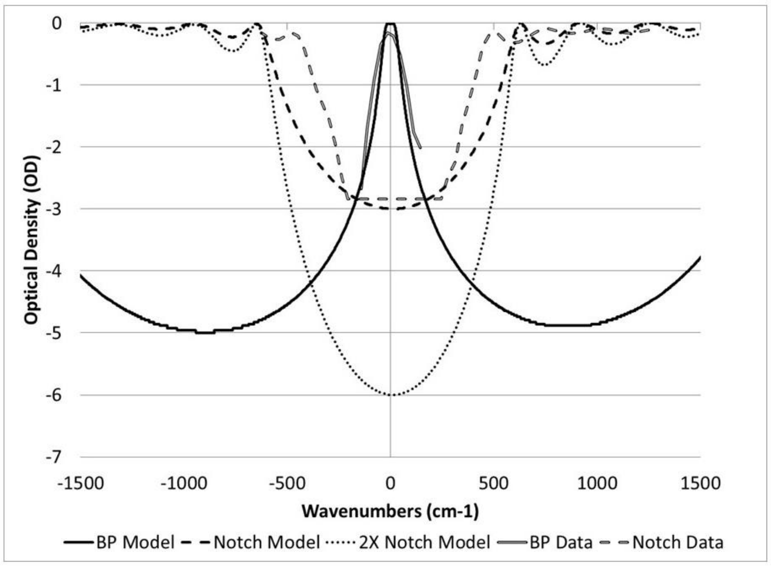

Figure 2. OD versus wavenumber for e-beam evaporated coatings

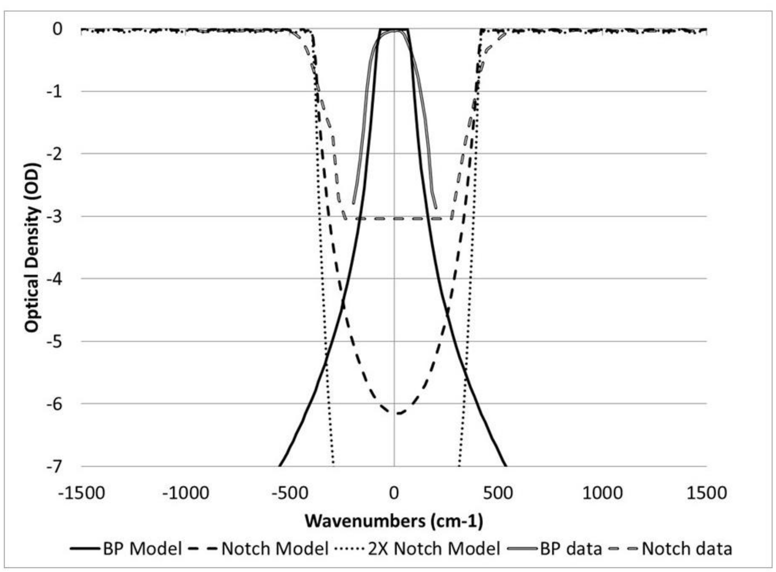

Figure 3. OD versus wavenumber for sputtered coatings

3. THIN FILM DEPOSITIONS

The e-beam depositions were performed under mid 10^{-5} torr vacuum levels (Barton et al. 2016) (Carver et al. 2015). The electron beam source allows for a denser and more robust filter than standard thermal sources. Coatings were deposited on the FC/PC connector tips of multimode fiber with NA = 0.21, and a core size of 62.5 micron. The deposition of each layer is controlled by monitoring the reflectance of the tip during growth. This is done by directing monochromatic light through a fiber feed-through into the vacuum system. The reflected light from the tip is collected with a beam splitter and sensed with a power meter. Cut points after each layer is complete are manually found by observing oscillations in the displayed run trace. In-situ monitoring of the growing filter enables the system to adjust to the sticking coefficient of the fiber tips – often different than the sticking coefficient of glass substrates.

The sputtered depositions were performed in one of our high-volume plasma assisted reactive magnetron sputtering (PARMS) systems. Unlike traditional physical vapor depositions that evaporate starting materials, PARMS bombards an elemental target (usually Si or Nb) using a magnetically accelerated argon/oxygen plasma. The accelerated atoms transfer momentum to the target material which in turn ejects the material from the surface onto the substrates, forming a thin sub-monolayer. The substrates rotate through a different part of the chamber where an oxygen plasma oxidizes the newly formed atomic layer, creating an oxide. The resulting thin-film layers are very dense and durable. Optical monitoring is performed as the monitor plate rotates through the beam. The system is automatically monitored in real-time so high reproducibility can be maintained. The same fibers used above are positioned such that the tips encounter the same flux as the monitor beam.

4. OPTICAL PERFORMANCE

Transmission of the coated tips was tested with a customized system composed of a bank of light emitting diodes (LEDs), a monochromator, and a power meter. The test set has a spectral resolution of one nanometer and can only measure down to OD3 due to available light intensity (where the OD curves are flat). Figures 2 and 3 also show data acquired on this test set for the e-beam and sputtered filters respectively. The e-beam bandpass has a peak transmission of 69% and roughly follows the modeled beam shape. The largest peak in the laser-induced fiber Raman signal is in the 400 to 600 cm^{-1} range. Blocking this signal is required to reduce background during Raman spectroscopy. The narrow-bandpass model indicates OD4 to OD5 blocking in this region. The measured e-beam notch blocks the laser to about OD3 but poorly follows the modeled shape due to the manual nature of the e-beam system. Coating both ends of the collection fiber will provide about OD6 blocking at the laser wavelength. Useful transmission with significant ripple is observed in the Stokes band above about 480 cm^{-1}. The sputtered bandpass has a peak transmission of 94% and roughly follows the modeled beam shape. Blocking of the peak fiber Raman band is expected to range from OD5.5 to OD7.5. The sputtered notch should block the laser to about OD6 and roughly follows the modeled shape due to the automated nature of the PARMS system. Coating both ends of the collection fiber will provide about OD12 blocking at the laser wavelength. Useful transmission with minimal ripple is observed in the Stokes band above about 480 cm^{-1}.

Coated fibers similar to those depicted in figure 2 were also tested using a compact, benchtop Raman setup. A fiber-coupled, multimode laser diode operating near 519 nm was used as the light source for the Raman measurements. The laser produces > 100 mW of optical power and requires a compliance voltage of less than 7 volts with an applied current of 300 mA. The laser spectrum was measured and the multimode output of the diode emits on several adjacent wavelengths that span ~ 2 – 3 nm, thus limiting the resolution of the Raman measurements. The laser as mounted in a temperature-controlled laser diode mount to account for the lack of a thermoelectric cooler in the diode package, and the mount temperature was controlled by a Thorlabs ITC 4001. Laser current was provided by a Wavelengths Electronics

LDTC 1020. The Raman scatter was focused onto the fiber and detected by a Thorlabs CCS 200 extended range compact spectrometer in both back and side-scattering configurations. This spectrometer is fiber-coupled and includes a grating that is reasonably efficient over the target wavelengths. However, the CCD array in the spectrometer is not cooled, limiting the noise of the Raman system. Figure 4a shows a measured Raman scattering spectrum of an acrylic block taken in the side-scattering configuration using the aforementioned laser fiber bandpass and collection fiber notch filters. The published spectrum is shown in Figure 4b and the strong feature near 3000 cm^{-1} is clearly indicated on both spectra. Note that the spectrometer noise and resolution of our early the test setup was too large to observe any of the smaller features.

5. DISCUSSION

In the e-beam method, the narrow bandpass (in the 780-790 nm region) is slightly lower transmitting and wider in wavelength than the model. The two-cavity model provides a small flat-top region for high performance over a small AOI range. The multicavity PARMS bandpass provides a larger flat-top region with steeper edges and higher out-of-band blocking. It also exhibits higher peak transmission than the e-beam filter. Using the manual e-beam process, we have demonstrated notch blocking down to 480 cm^{-1} with high out of band transmission. Deeper blocking can be achieved by applying the same coating to both ends of the fiber. The e-beam method has a coating thickness limit of roughly 7 microns which reduces the amount of blocking we can achieve on one end of the fiber. The thickness limit also restricts our ability to reduce ripple in the transmitting region. In contrast, the PARMS method enables blocking down to OD 6 on a single tip with low ripple in the transmitting region. The PARMS notch filter also allows detection to roughly 480 cm^{-1}. Differences between the models and measured values are due to small errors between the actual refractive indices and those used in the model and the fact that these tips are measured in a system that samples the full NA of the fiber. The models in the figures only illustrate performance at an AOI of zero.

The Raman spectra using our fiber tips given in figure 4 show the polymer C-H stretch bands around 3000 cm^{-1} for a polymethylmethacrylate sample. Based on the above OD plots and this early Raman spectra, our coated fiber tips will be sufficient to detect a majority of peaks in the regions of interest for biological sensing, including most of the fingerprint region from 500-1500 cm^{-1} using both Stokes and anti-Stokes detection simultaneously. Some biologically interesting applications include blood glucose monitoring (550-1680 cm^{-1}) and cancer detection (2900-3600 cm^{-1}). We anticipate that as the project progresses, we will more closely approximate the results of the models, especially using the PARMS system. Further, switching to a long-pass/short-pass configuration will allow us to observe Raman scatter down to 200 cm^{-1}. We have already demonstrated PARMS coatings on fiber tips with a 10 nm wide transition from a transmission of 10% to 90% using a physical thickness of 22 microns.

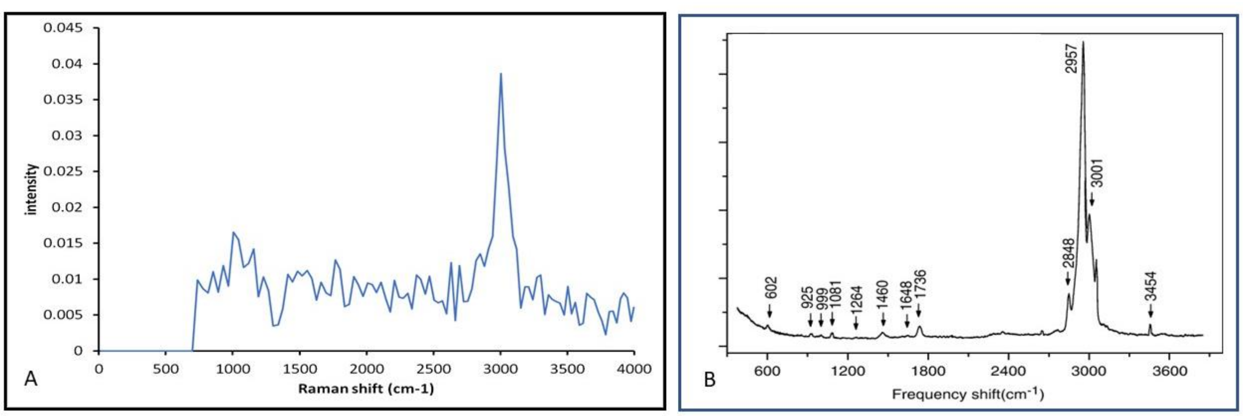

Figure 4. A. Raman spectrum of an acrylic block using a 519 nm laser line filter and notch combination on two separate fiber tips. **B.** Reference spectrum of an acrylic block (Thomas et al. 2008)

6. CONCLUSIONS

We have demonstrated the application of steep notch and narrow band filters to the ends of individual fiber tips using both e-beam and PARMS deposition methods. Measurements indicate that the filters maintain their spectral fidelity despite an AOI range of 12 degrees. We have demonstrated that Raman spectra can be obtained using these individual tips. Next, we will develop a patterning method for coating fiber tip bundles with different types of filters and add focusing optics to develop a full probe. This probe will be deployed into a single-point measuring device for biomedical applications such as surgical margin guidance, glucose monitoring, or optical biopsy. We are also translating the fiber tip deposition process into a high volume production scenario.

ACKNOWLEDGEMENTS

We thank Dr. Bob Johnson of Omega Optical for supporting this effort.

REFERENCES

[1] Kauffmann, T.H., Kokanyan, N., Fontana, M.D., "Use of Stokes and anti-Stokes Raman scattering for new applications," Journal of Raman Spectroscopy 50 (3), 2019, pp.418-424. DOI: org/10.1002/jrs.5523

[2] Singh, S.P., Gangwar, R., Singh, N., "Nonlinear Scattering Effects in Optical Fibers," Progress in Electromagnetics Research, PIER, 379-405, 2007 DOI: 10.2528/PIER07051102

[3] Barton, J.B., Chanda, S., Locknar, S.A. and Carver, G.E., "Coated fiber tips for optical instrumentation", Proc. SPIE 9754, Photonic Instrumentation Engineering III, 97540D (March 16, 2016); doi:10.1117/12.2211083

[4] Carver, G.E., Chanda, S.K., Morrison, W.A., Locknar, S.A. and Johnson, R.L. "System for multispectral imaging of fluorescence", US Patent # 9,155,474 (October 13, 2015)

[5] Thomas, K.J., Sheeba, M., Nampoori, V.P.N., Vallabhan, C.P.G. and Radhakrishnan, "Raman spectra of polymethyl methacrylate optical fibres excited by a 532 nm diode pumped solid state laser," Journal of Optics A: Pure and Applied Optics, 10(5), p.055303, 2008.